Cellular Oncology (2023) 46:1855–1870
https://doi.org/10.1007/s13402-023-00860-3

RESEARCH

Triggering pyroptosis enhances the antitumor efficacy of PARP inhibitors in prostate cancer

Ao Tian[1] · Tingyu Wu[1] · Yanshuang Zhang[1] · Jiachen Chen[1] · Jianjun Sha[2] · Weiliang Xia[1]

Accepted: 5 August 2023 / Published online: 23 August 2023
© Springer Nature Switzerland AG 2023

Abstract

Purpose PARP inhibitors have revolutionized the treatment landscape for advanced prostate cancer (PCa) patients who harboring mutations in homologous recombination repair (HRR) genes. However, the molecular mechanisms underlying PARP inhibitors function beyond DNA damage repair pathways remain elusive, and identifying novel predictive targets that favorably respond to PARP inhibitors in PCa is an active area of research.

Methods The expression of GSDME in PCa cell lines and human PCa samples was determined by western blotting. Targeted bisulfite sequencing, gene enrichment analysis (GSEA), clone formation, construction of the stably transfected cell lines, lactate dehydrogenase (LDH) assay, western blotting as well as a mouse model of subcutaneous xenografts were used to investigate the role of GSDME in PCa. The combinational therapeutic effect of olaparib and decitabine was determined using both in vitro and in vivo experiments.

Results We have found low expression of GSDME in PCa. Interestingly, we demonstrated that GSDME activity is robustly induced in olaparib-treated cells undergoing pyroptosis, and that high methylation of the GSDME promoter dampens its activity in PCa cells. Intriguingly, genetically overexpressing GSDME does not inhibit tumor cell proliferation but instead confers sensitivity to olaparib. Furthermore, pharmacological treatment with the combination of olaparib and decitabine synergistically induces GSDME expression and cleavage through caspase-3 activation, thus promoting pyroptosis and enhancing anti-tumor response, ultimately resulting in tumor remission.

Conclusion Our findings highlight a novel therapeutic strategy for enhancing the long-term response to olaparib beyond HRR-deficient tumors in PCa, underscoring the critical role of GSDME in regulating tumorigenesis.

Keywords GSDME · Olaparib · Pyroptosis · Decitabine · Prostate cancer

Ao Tian and Tingyu Wu contributed equally to this work.

✉ Weiliang Xia
wlxia@sjtu.edu.cn

Ao Tian
tianao60@sjtu.edu.cn

Tingyu Wu
wutingyu@sjtu.edu.cn

Yanshuang Zhang
yanshuangzhang@126.com

Jiachen Chen
chenjiachen@sjtu.edu.cn

Jianjun Sha
shajianjunrj@126.com

[1] State Key Laboratory of Systems Medicine for Cancer, Renji Hospital, School of Medicine and School of Biomedical Engineering, Shanghai Jiao Tong University, 1954 Huashan Road, Shanghai 200030, China

[2] Department of Urology, Ren Ji Hospital, School of Medicine, Shanghai Jiao Tong University, 145 Shandong Middle road, Shanghai 200001, China

1 Introduction

Androgen deprivation therapy (ADT) remains a crucial therapeutic modality for PCa, which is one of the most prevalent malignancy and cancer-related cause of mortality among men [1, 2]. Although many patients initially respond positively to ADT and second-generation antiandrogen drugs like enzalutamide, abiraterone, and apalutamide, they often develop resistance to these treatments, leading to recurrent malignant tumors and refractory metastatic castration-resistant prostate cancer (mCRPC) [3, 4]. Hopefully, approximately 30% of patients harbor deleterious mutations in DNA damage repair (DDR) genes, conferring the possibility of targeting poly-ADP-ribose polymerase (PARP), a crucial enzyme involved in DNA repair [5, 6]. Olaparib, an FDA-approved PARP1 inhibitor, has shown significant improvements in overall survival and prognosis for mCRPC patients possessing at least one of the 15 prespecified genes that play a direct or indirect role in homologous recombination repair (HRR) [7, 8]. Regrettably, PARP inhibitors' response typically only lasts for a short duration, and eventual acquired resistance can result in fatal patient outcomes [9]. Reinforcing the long-term efficacy of PARP inhibitors remains a significant challenge, requiring the exploration of alternative strategies to enhance the prolonged antitumor effects of PARP inhibitors such as olaparib.

GSDME, also known as DFNA5, is located on human chromosome 7pl5 and its mutation results in hearing impairment [10]. Evidence in recent years has shown that it is a member of the gasdermins family that mediates pyroptosis, a form of regulated cell death (RCD) distinct from apoptosis [11]. Caspase-3 was previously thought to be the main effector of apoptosis, but increasing evidence has also shown that caspase-3-mediated GSDME cleavage, an essential step to produce pyroptosis, which can also repress tumor growth by activating anti-tumor immune responses or other mechanisms [12, 13]. Altogether, the induction of pyroptosis is likely to be a potent intervention for targeting tumors. However, GSDME is frequently silenced by epigenetic mechanisms in various cancers, which is associated with poor prognosis. The CpG islands in the promoter region of the gene are highly methylated, which may contribute to its silencing [14–16]. GSDME was previously reported to be expressed in PCa [17, 18]. Whether GSDME acts as a crucial factor in the progression of PCa by being epigenetically silenced remains to be elucidated.

Preclinical evidence suggests that increasing the expression level of GSDME can induce pyroptosis and have anti-carcinogenic effects. For example, overexpression of GSDME suppressed proliferation by inducing cell cycle arrest in hepatocellular carcinoma cells [19]. Although GSDME is expressed as a tumor suppressor in various cancers, it is often maintained at low levels due to DNA methylation. There are reliable evidences that the promoter DNA methylation can be inhibited by 5-aza-2'-deoxycytidine (decitabine), an FDA-approved inhibitor of DNA methyltransferases that has demonstrated efficacy in hematological neoplasms and breast cancer [20, 21]. According to this characterization, decitabine induces demethylation and restores GSDME expression. In this context, restoration of GSDME sensitivity via decitabine also enhances the response of tumor cells to standard chemotherapeutic agents, such as doxorubicin, actinomycin-D, and etoposide, by predisposing them to pyroptosis [13, 22]. Thus, targeting GSDME and its downstream pathways through decitabine-induced demethylation may represent a promising strategy for enhancing the effects of standard chemotherapy and promoting pyroptosis in cancer cells.

In this study, we report that the expression of GSDME is significantly reduced in PCa cell lines and tissues. Leveraging a quantitative DNA methylation assay and next-generation sequencing (NGS) technology, we were able to detect aberrant methylation of the GSDME promoter in 22Rv1 and PC3 cells. Our results demonstrate that GSDME displays frequent epigenetic activation in both cell lines and databases, which is significantly correlated with poor prognosis. Notably, olaparib activates caspase-3 to cleave GSDME, which initiates pyroptosis in PCa cell lines. Additionally, our data show that the combination of olaparib and decitabine induces a more potent antitumor effect both in vitro and in vivo. Taken together, our study highlights the potential for a combined treatment strategy involving pyroptosis induction as a promising approach for the clinical management of PCa.

2 Materials and methods

2.1 Cell lines and cell culture

The human PCa lines 22Rv1, C42B, DU145 and H660 were purchased from the Cell Resource of Shanghai Institute of Biological Sciences, Chinese Academy of Sciences (Shanghai, China). PC3 and benign prostatic hyperplasia cell line (BPH-1) were obtained from Dr. Wei-Qiang Gao (Clinical Stem Cell Center, Ren Ji Hospital, School of Medicine, Shanghai Jiao Tong University). LNCaP (CL-0143) and WPMY-1 (CL-0467) were kindly provided by Procell Life Science &Technology Co., Ltd. The BPH-1, PC-3, 22Rv1 and LNCaP were cultured in RPMI-1640 medium (RPMI, Hyclone). The C42B, DU145, H660 and WPMY-1 were cultured in Dulbecco's modified Eagle's medium (DMEM, Hyclone). All cell culture s were supplemented with 10% heat inactivated fetal bovine serum (FBS, Gemini). All cells

were cultured at 37 °C in a humidified environment with 5% CO_2.

2.2 Gene expression and methylation profiles

Relative mRNA levels of GSDME of Wallace Prostate, Welsh Prostate and Yu Prostate cohorts were downloaded from the Oncomine database. The RNA-seq data and the methylation levels of GSDME of the TCGA-PRAD were downloaded from the TCGA database (https://portal.gdc.cancer.gov/) and the human disease methylation database (http://bio-bigdata.hrbmu.edu.cn/diseasemeth/). RNA-seq data were analyzed by gene sets enrichment using GSEA software [23, 24]. The microarray datasets of GSE74013, GSE6919, GSE8511 and GSE38241 were downloaded from the GEO database (https://www.ncbi.nlm.nih.gov/geo/). Linear regression correlations between the mRNA levels of GSDME and the methylation mean beta value of promoter of GSDME were conducted from DNA Methylation Interactive Visualization Database (DNMIVD) [25]. Prognostic values of the methylation levels of GSDME were analyzed to obtain the Kaplan-Meier survival curves for PRAD patients, using DNMIVD and EWAS Data Hub database [26].

2.3 Clinical sample

Fresh biopsy samples including benign prostatic hyperplasia (n = 7) and PCa (n = 7) were obtained from Ren Ji Hospital, School of Medicine, Shanghai Jiao Tong University. Ethics committee approval from School of Biomedical Engineering, Shanghai Jiao Tong University was obtained prior to the research (BME-2,017,032) and informed written consent of all participants were obtained.

2.4 Immunohistochemistry

The tissue microarray (TMA) (#PR8011a) containing 8 normal prostate tissues, 26 prostate hyperplasia tissues, and 32 PCa tissues was purchased from US Biomax (Derwood, MD). GSDME staining intensity of TMA was scored into extremely positive (+++), strongly positive (++), positive (+) and weakly positive (-) categories. Briefly, tissue microarrays were placed at 62 °C for 1 h. Tissue microarrays were dewaxed and rehydrated in xylene and stepwise dilution of ethanol. Endogenous peroxidase activity was blocked by adding 100 µl of hydrogen peroxide blocking solution dropwise for 10 min at room temperature, followed by antigen repair using Tris-EDTA (pH = 9.0). After incubation with 5% BSA at room temperature for 20 min, samples were incubated with GSDME primary antibody (Proteintech, 13075-1-AP) at 4 °C overnight. The next day, the samples were washed 3 times with PBS and incubated with the labeled secondary antibody for 30 min at 37 °C. Then, DAB solution was dropped and the samples were re-stained with hematoxylin for 30 s. The final coverslip was covered with neutral resin on the sample and observed under the microscope.

2.5 Evaluation of methylation levels in cell lines

The promoter sequence of the GSDME gene was acquired from NCBI, and the core promoter (7:24796400–24,797,601), and the flanking region (7:24795602–24,798,199) were reported to be considered as putative promoters of DFNA5 [27]. In our study, the core promoter region (7:24796400–24,797,601) of GSDME was examined for methylation with targeted next-generation bisulfite sequencing analysis. The procedures included four steps: sample preparation, sulfite treatment, PCR amplification and NGS sequencing. In a nutshell, cells ($> 1 \times 10^6$ cells) were separately purified for genomic DNA using the Ezup Column Animal Tissue Genomic DNA Extraction Kit (Sangon Biotech, B51821), and the concentration of the mentioned genomic DNA was measured using a UV-Vis spectrophotometer (Merinton, Sma4000). Bisulfite convert up to 500 ng (or maximum of 20 µL) nucleic acid samples. All samples were treated using EZ DNA Methylation-Gold kit (Zymo Research, D5005), according to the manufacturer's instructions. PCR reactions were used to amplify all Bisulfite modified DNA samples. The PCR reactions consisted of 5 µL of Taq Plus DNA polymerase (Sangon Biotech, B600090), 4 µL of primers and 1 µL of Bisulfite-treated DNA samples in a 50 µL system. The PCR setting procedure consists of pre-denaturation at 95 °C for 3–5 min, followed by 95 °C for 30 s, the specific annealing temperature of each primer at 55 °C for 30 s, extension at 72 °C for 30 s, 68 °C for 30 s for 35 cycles, and final repair extension at 72 °C for 5 min. After the reaction, 5 µL of PCR products were taken on a 1% agarose gel (Sangon Biotech, A500016) for electrophoresis and agarose gel containing the target bands was collected. Finally high-throughput sequencing was performed using an instrument (Illumina, Miseq) and FastQ data were obtained. The data were analyzed according to methods that have been published in the literature. Methylation levels were calculated by dividing the number of sites where methylation occurred by the total number of methylated sites [28, 29]. PCR primers for the GSDME promoter (MN957-1-forward GYGGTTTTGGAAAGGGTTA, MN957-1-reverse ATCCCCTTCCCATCCTCTC; MN957-2-forward AGGATGGGAAGGGGATGTT, MN957-2-reverse AACCCTCTCTCCRCCCTC; MN957-3-forward GGGAGGGYGGAGAGAGG, MN957-3-reverse AATCCACACTCCACTATAAATAACRA; MN957-4-forward

TYGTTATTTATAGTGGAGTGTGGAT, MN957-4-reverse ACACCCAATATATAAA.

AACRCCTA) were designed by Sangon Biotech.

2.6 Protein lysate preparation and western blotting (WB)

The protein immunoblots were presented to detect the expression levels of different proteins in different samples as described previously [30]. Total proteins of cells or tissues were extracted by RIPA lysis buffer containing protease inhibitor, phosphatase inhibitor and phenylmethyl sulfonyl fluoride. The protein concentration of each sample was determined using the BCA kit (Thermo, 23227), with the indicated standards as the references. The equal amounts of denatured proteins were loaded in 10% or 12.5% SDS-PAGE for 80 min at a constant 120 V and transferred to nitrocellulose membranes after electrophoresis at a constant 300 mA for 90 min. Membranes were blocked with skim milk buffer for 1 h at room temperature and washed 3 times. Membranes were incubated overnight at 4 °C with the following primary antibodies, GSDME (Abcam, ab215191), GSDMB (Abcam, ab215729), GSDMD (CST, 39754 S), PARP (CST, 9532 S), caspase-3 (CST, 9662 S), cleaved caspase-3 (CST, 9664 S), Survivin (CST, 2808 S), BCL-2 (Abcam, ab182858), GAPDH (Proteintech, 60004-1-Ig), β-Tubulin (Proteintech, 66240-1-Ig). Membranes were washed 3 times with TBST buffer containing 1% Tween, and were incubated with appropriate horseradish peroxidase-conjugated anti-mouse or anti-rabbit secondary antibodies for 1 h at room temperature. In the end, immunoblots were visualized using a chemiluminescent imaging system (Tanon, 5200). The intensity values of the protein blots were quantified and analyzed using ImageJ software.

2.7 Apoptosis analysis by flow cytometry

Annexin V^+ cells were analyzed by flow cytometry as previously described [31]. Briefly, the cells were treated at the indicated concentrations and time points, the medium for each group was collected, the cells were trypsin digested, and washed once with PBS. After cells were centrifuged, apoptosis levels were measured using the PE Annexin V Apoptosis Detection Kit I (BD Pharmingen). Cells were resuspended with 1×Binding Buffer, transferred to flow tubes. 5 μL of PE Annexin V and 5 μL of 7-AAD were added per tube, cells were gently vortexed and incubated at room temperature protected from light for 15 min, the reaction was terminated using 400 μL of 1×Binding Buffer, and samples were analyzed using a flow cytometer (FACS Aria II, BD Biosciences). All groups of data were analyzed by FlowJo software.

2.8 Cell viability assay

Proliferating cells were trypsin digested, centrifuged, resuspended, and counted. For proliferating or dosed cells, 5000 cells per well were planted in 96-well plates, cells were cultured at 37 °C with 5% CO_2 for 24 h. After cells were treated with fresh complete medium containing different indicated doses of olaparib and decitabine for 96 h, and finally cell viability in each panel was determined using the CCK − 8 assay kit.

2.9 LDH assay

The following solutions were prepared: the 50× lysis buffer consisted of 49 mL ddH_2O, 1 mL Triton X-100, 0.25 g BSA and 1.19 g HEPES. The LDH buffer contains 500 ml ddH_2O, 17 g KH_2PO_4 and 21.8 g K_2HPO_4. LDH reaction buffer was prepared from 20 mL LDH buffer, 0.5 mL 100 nM pyruvate and 5 mg NADH. The pH value of the mentioned solution is adjusted to 7.5. The cell culture medium was collected for the detection of extracellular LDH. 300 μL of Lysing buffer was added to the cells in a 24-well plate, and the plate was shaken vigorously on a shaker for 20 min. Add 50 μL of the cell culture supernatant (extracellular LDH)/lysed cytosol (intracellular LDH) to each well in a 96-well plate. The LDH reaction buffer was added rapidly at once, 200 μL per well, and the absorbance value at 340 nm was read immediately with an enzyme marker at 5 s intervals for 30 s. The maximum reaction rate was calculated from the absorbance value, and the reaction rate characterized the activity of LDH.

2.10 Lentiviral infection and construction of stable transfected cell lines

The GSDME overexpression lentivirus was constructed by GENECHEM Biotechnology Co. Ltd. (Shanghai, China). Cells were stably transfected with lentivirus through 2 μg/mL puromycin selection.

2.11 Colony formation assay

For pharmaceutical treatments, the proliferating cells were trypsin digested, centrifuged, resuspended, and counted, 1×10^5 cells were planted in 6-well plates and cultured for 24 H. After treatment with the indicated concentrations of fresh medium containing the drugs for 96 h, cells were fixed in 4% paraformaldehyde and stained with 0.1% crystal violet, and clones of cells per well were quantified and analyzed using ImageJ software. For the stably transfected cell lines, cells were transfected with GSDME-OE lentivirus or control lentivirus, and the equivalent number of cells were

planted in 6-well plates and cultured for 96 h. The following steps were performed as described above.

2.12 Subcutaneous tumorigenesis model and in vivo treatment

Cell-derived xenograft model was generated as previously described [32]. In brief, proliferating 22Rv1 cells were trypsin digested, centrifuged, resuspended, and counted, and 5×10^{6} cells were resuspended in 100 μL PBS buffer with 1% Matrigel (Corning, 354,248) were injected into the right flank region of 6-week-old immunodeficient nude male mice, and tumor volume and mouse weight were observed once every 3 days. On day 14 post injection when the tumor grew to 50–100 mm^3, mice were randomly assigned to groups, and on day 15 treatment was administered once daily and given an equal volume of saline (i.p.), olaparib (50 mg/kg, i.p.) and/or decitabine (50 μg/g, i.p.). Tumor volume was measured daily using vernier calipers and calculated using tumor volume = ½ length × $width^2$. After 15 days of treatment, the mice were sacrificed to be prepared as ex vivo samples for subsequent experimental analysis. The animal model experiments were approved by the Research Ethics Committee of the School of Biomedical Engineering, Shanghai Jiao Tong University.

2.13 Statistical analysis

All the graphical significance is indicated by * $p < 0.05$, ** $p < 0.01$, *** $p < 0.001$, **** $p < 0.0001$, and when $p > 0.05$ was defined as no significant (ns) difference between the two groups. Comparisons between the two groups are statistically determined by two-tailed unpaired or paired t-tests and One-way ANOVA is used to compare three or more experimental groups using GraphPad prism 7.0 software. The number of animal samples and patient cohorts (n) is shown in each plot. The data are displayed as box plots, where the middle line shows the mean of the samples, the upper and lower bounds represent the upper quartile and lower quartile, respectively, and the error values extend to the maximum and minimum values, and points outside the box plots are considered outliers that are outside the bounding range. Error bars are expressed as means ± SEM.

3 Results

3.1 Epigenetic silencing of GSDME is a predictor for poor prognosis in PCa

To further investigate the role of GSDME in PCa, we obtained RNA-seq data from multiple published datasets of PCa cohorts, and analyzed the expression levels of GSDME in these samples. Using the Oncomine database, we compared the variation of GSDME expression in normal and cancerous prostate tissue cohorts, and found that the expression levels of GSDME were significantly reduced in multiple PCa cohorts when compared to normal prostate tissue (Fig. 1a). These findings are consistent with our other results analyzing a PRAD cohort from the TCGA database (Fig. 1b), which strengthens the conclusion that GSDME may play an important role in PCa progression. Furthermore, we investigated the expression levels of GSDME in metastatic tissues using additional datasets from the GEO database (Supplementary Fig. S1a). We observed that GSDME expression was also lower in metastatic tissues, suggesting that the downregulation of GSDME might be associated with the malignant phenotype of PCa. Overall, our findings indicate that GSDME may serve as a promising biomarker for the diagnosis and prognosis of PCa.

A growing body of evidences demonstrate that methylation of the GSDME gene is frequently detected in breast and colorectal cancer, suggesting that GSDME promoter methylation may serve as a novel biomarker for diverse cancers [33, 34]. In view of this, we hypothesized that the low expression of GSDME in PCa might be attributed to DNA epigenetic silencing. To determine whether the downregulation of GSDME is correlated with enhanced methylation of its promoter in PCa, and we analyzed two cohorts from TCGA and GEO databases and found upregulated levels of methylation of GSDME in PCa (Fig. 1c, Supplementary Fig. S1b). These findings suggest that abnormalities in the methylation process of specific genes may contribute to the lower expression of GSDME in PCa tissues. Our analysis further revealed that the expression level of GSDME was significantly and negatively correlated with the degree of promoter methylation in TCGA-PRAD cohorts (Fig. 1d, Supplementary Fig. S1c). Moreover, survival curves from the Kaplan-Meier plotter showed that higher methylation of GSDME was associated with shorter disease-free intervals (DFI) and overall survival (OS) (Fig. 1e, Supplementary Fig. S1d). To validate our above results, we examined the GSDME protein levels in a panel of PCa and prostate cell lines, including androgen-dependent (LNCaP), androgen-sensitive (22Rv1), androgen-independent (C42B, PC3, DU145), neuroendocrine-type (H660), human benign prostatic hyperplasia (BPH-1) and prostate stromal (WPMY-1) cell lines, and found that GSDME protein levels were decreased in PCa cell lines compared to BPH-1 and WPMY-1 cell lines (Fig. 1f). We evaluated IHC staining for GSDME in a prostate-associated tissue microarray containing 8 normal prostate, 26 prostate hyperplasia and 32 PCa tissues, and showed that GSDME was significantly low expressed in PCa tissues (Fig. 1g). Consistently, lower

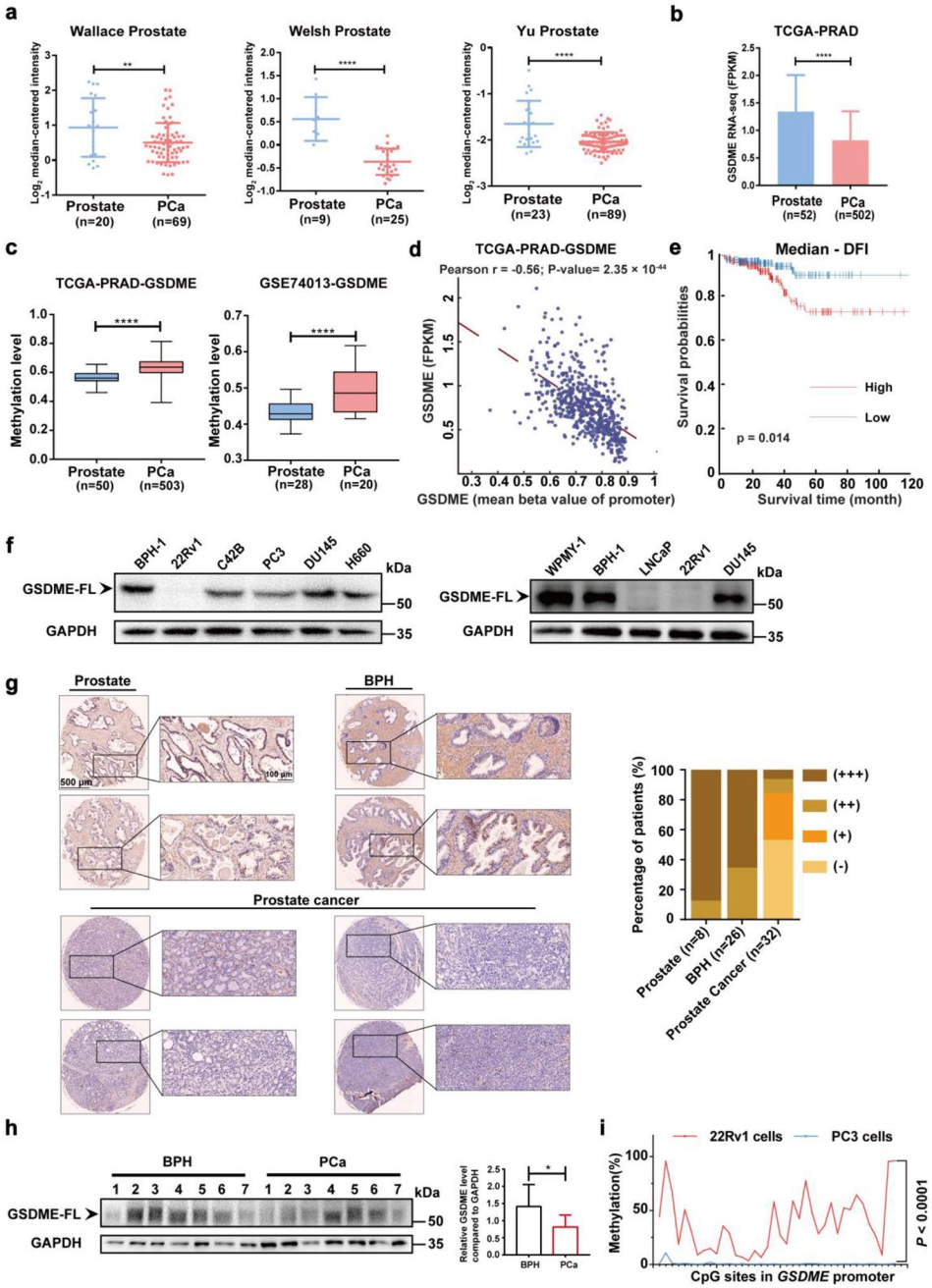

Fig. 1 GSDME is low expressed in human PCa cell lines and tumor samples, and higher methylation of promoter is correlated with poor prognosis. **(a)** Expression of GSDME and copy number analyses of GSDME in Wallcae Prostate, Welsh Prostate and Yu prostate cohorts from Oncomine database. **(b)** The transcription level of GSDME in a PRAD (n = 502) cohort and a normal cohort (n = 52) from TCGA Research Network (https://cancergenome.nih.gov/). **(c)** The methylation level of GSDME in normal prostate tissue and PRAD from TCGA and GEO (GSE74013) database. **(d)** Pearson's correlation between the transcription level and methylation level of GSDME in PRAD cohorts from TCGA and was analyzed at DNA Methylation Interactive Visualization Database (DNMIVD). **(e)** Kaplan–Meier plot of the PCa patients for disease-free interval (DFI) was represented in which patients were stratified by the methylation level of GSDME from TCGA database at DNMIVD. **(f)** Representative western blots on the protein expression of GSDME in WPMY-1, BPH-1 and human PCa cell lines (LNCaP, 22Rv1, C42B, PC3, DU145 and H660). **(g)** Representative IHC of GSDME expression in a PCa tissue array. (Prostate, n = 8; BPH, n = 26; Prostate cancer, n = 32). **(h)** The protein expression of GSDME in prostate biopsy samples (left) and quantification (right). n = 7 for BPH tissues and n = 7 for PCa tissues. **(i)** The locations of representative 38 CpG sites analyzed in the GSDME promoter and the percentage of methylation on each CpG site as determined by bisulfite sequencing of 22Rv1 and PC3 cells. The p value was determined two-sided paired t-test. Error bars are expressed as means ± SEM, $*p < 0.05$, $**p < 0.01$, $****p < 0.0001$

levels of GSDME protein expression were detected in prostate biopsy samples, including benign prostatic hyperplasia (BPH) (n = 7) and PCa (n = 7) by western blot (Fig. 1h).

To examine whether GSDME expression is regulated by DNA methylation in different cell lines, we conducted targeted next-generation bisulfite sequencing analysis on the GSDME promoter. We found that nearly all CpG sites in these representative regions showed the higher levels of DNA methylation in 22Rv1 cells when compared to PC3 cells in culture (Fig. 1i). Taken together, these findings suggest that the protein expression level of GSDME may be determined by epigenetic factors and correlates with the prognosis of patients with PCa.

3.2 Therapy-induced pyroptosis restrains the proliferation of PCa cells

To gain further insights into the role of GSDME in PCa, we conducted an in-depth transcriptomic analysis of a PRAD cohort from the TCGA database. Our analysis revealed that multiple gene signatures associated with PCa were significantly enriched in samples with low expression of GSDME, which indicated that GSDME downregulation may contribute to prostate carcinogenesis (Fig. 2a, Supplementary Fig. S2a). Remarkably, our results also uncovered a significant enrichment of the pyroptosis signaling pathway gene signature in the high-expression GSDME cohort, which implied

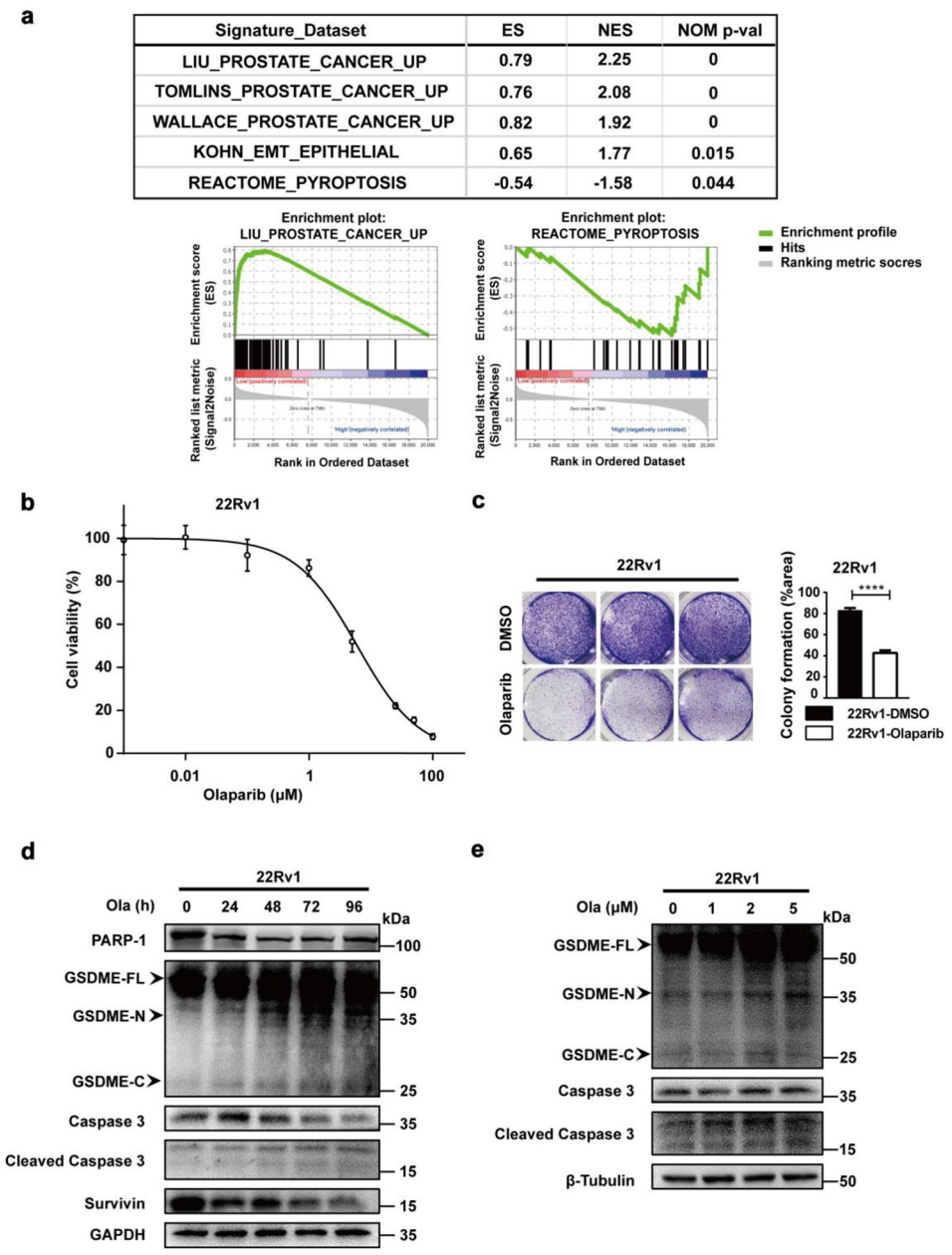

Signature_Dataset	ES	NES	NOM p-val
LIU_PROSTATE_CANCER_UP	0.79	2.25	0
TOMLINS_PROSTATE_CANCER_UP	0.76	2.08	0
WALLACE_PROSTATE_CANCER_UP	0.82	1.92	0
KOHN_EMT_EPITHELIAL	0.65	1.77	0.015
REACTOME_PYROPTOSIS	-0.54	-1.58	0.044

Fig. 2 Therapy-induced pyroptosis blocks the growth of 22Rv1 cells in vitro. **(a)** RNA sequencing was performed on PRAD cohorts with GSDME low versus high expression for multiple independent signaling pathway gene sets by GSEA from TCGA database. Low (n = 251), High (n = 251). **(b)** Dose-response curves after treatment with olaparib as indicated for 7 days in 22Rv1 cells. **(c)** The colony formation assay was performed over 96 h after treatment with 10 μM olaparib on 22Rv1 cells (left) and quantification (right). **(d)** Proteins were extracted from 22Rv1 cells, treated with 5 μM olaparib for 0, 24, 48, 72 and 96 h and then analyzed by western blotting respectively. **(e)** Proteins were extracted from 22Rv1 cells, treated with 0, 1, 2 and 5 μM doses of olaparib for 96 h and then analyzed by western blotting respectively. Error bars are expressed as mean ± SEM, two-sided unpaired t-test, ****$p < 0.0001$

that the GSDME-mediated pyroptotic program might be unexpectedly suppressed and promote PCa development in patients with reduced levels of GSDME (Fig. 2a, Supplementary Fig. S2b).

Given that approximately 30% of PCa patients harbor mutations in at least one HRR gene within a cohort of 1013 patients [35], which confers susceptibilities to targeted therapies, such as olaparib (a PARP inhibitor) blocks tumor progression through synthetic lethality [6–8]. However, it has yet to be determined whether olaparib can mediate anti-tumor responses via alternative mechanisms in PCa. To investigate this, we analyzed the sensitivity of olaparib towards the AR-sensitive 22Rv1 cell line. We demonstrated that olaparib impeded the proliferation of 22Rv1 cells at micromolar concentrations based on a dose-response assay (Fig. 2b). Moreover, the inhibition of PARP enzymatic activity significantly impacted the growth of 22Rv1 cells, as evidenced by a colony formation assay (Fig. 2c). In order to identify potential alternative signaling pathways, we made an unexpected discovery that olaparib augmented the cleavage levels of GSDME protein in 22Rv1 cells, which became more pronounced with prolonged treatment (Fig. 2d). Given that activated caspase-3 governs the cleavage of the gasdermin-associated protein DFNA5, shifting of apoptosis to pyroptosis [22]. We observed that caspase-3 activation correlated with bulk cleavage of GSDME, rather than other gasdermins, and the consequent downregulation of survivin during treatment with olaparib (Fig. 2d, Supplementary Fig. S3a and 3b). Furthermore, we found that the activation of caspase-3 significantly increased in cleaving GSDME with dose escalation (Fig. 2e). Thus, our observations suggest that the anti-tumor effect of olaparib was mediated by pyroptosis in PCa cells, at least within this experimental context.

3.3 GSDME overexpression confers susceptibility to olaparib anti-tumor response in vitro

The interplay between GSDME and olaparib in PCa is an important emerging field of research. Lactate dehydrogenase (LDH) release is a key feature of the switch from apoptosis to pyroptosis [13]. Here, we reported that Olaparib led to a significant increase in GSDME cleavage and the release level of LDH in PC3 and DU145 cell lines, which are known to have relatively higher levels of GSDME expression than 22Rv1 cells (Figs. 1f and 3a). To further identify the role of GSDME in PCa, we constructed stably overexpressed GSDME in 22Rv1 cell lines (Fig. 3b) and tested the effect of GSDME overexpression on tumor cell proliferation. Our results showed that the proliferation rate of cells with GSDME overexpression didn't significant differences on control cell lines by clone formation and CCK-8 assay (Fig. 3c-d). Additionally, we also demonstrated that GSDME-OE cells were more sensitive to the anti-neoplastic response of olaparib, as evidenced by our experiments of varying olaparib doses to compare the sensitivity of control and GSDME-OE cell lines (Fig. 3e). Consistent with our hypothesis, substantial cells were induced towards the pyroptosis process in the overexpression of GSDME cells during response to olaparib. Moreover, considerably higher protein cleavage level of GSDME and the total release level of LDH had been occurred, along with the protein expression of survivin was significantly inhibited, in the overexpressed GSDME cells than control cells after olaparib treatment (Fig. 3f-g). Taken together, these results suggest that overexpression of GSDME confers a vulnerability profile that can be efficiently responded to olaparib, and the improvement in susceptibility is mediated by cleaving GSDME-induced pyroptosis in vitro. These findings shed light on the potential therapeutic implications of targeting GSDME as a mechanism to enhance the efficacy of PARP inhibitors such as olaparib in treating PCa.

3.4 Decitabine synergizes with olaparib to inhibit tumor growth via demethylation of GSDME in PCa cells

As previously reported, decitabine is a cytosine analogue and demethylating agent that irreversibly binds to the members of DNA methyltransferase family, which lead to the elevated expression of GSDME and the inhibition of tumor development [13, 36]. To investigate whether decitabine can enhance GSDME expression in 22Rv1 cells with low expression level of GSDME and inhibit hypermethylation in the promoter region, we evaluated the effect of different concentrations of decitabine on GSDME protein expression. After treatment with various concentrations (0, 0.1, and 0.5 μM) of decitabine, we showed that decitabine increased the expression of GSDME via a dose-dependent manner (Fig. 4a). We further explored single-agent as well as combination treatment strategies and found that the combination treatment significantly enhanced the level of pyroptosis in 22Rv1 cells (Fig. 4b). As expected, the combination treatment significantly decreased tumor proliferation compared to drug treatment alone by clone formation and CCK-8 assay (Fig. 4c, d). Then we quantified extracellular and intracellular LDH concentrations after single drug and combination treatments. Consistent with the above results, the combination treatment significantly increased extracellular LDH content (Fig. 4e). Additionally, we observed that the levels of cell apoptosis were not significantly increased in cells treated with olaparib and decitabine alone (Fig. 4f), which suggests that a subpopulation of cells may predispose to other forms of death, such as pyroptosis.

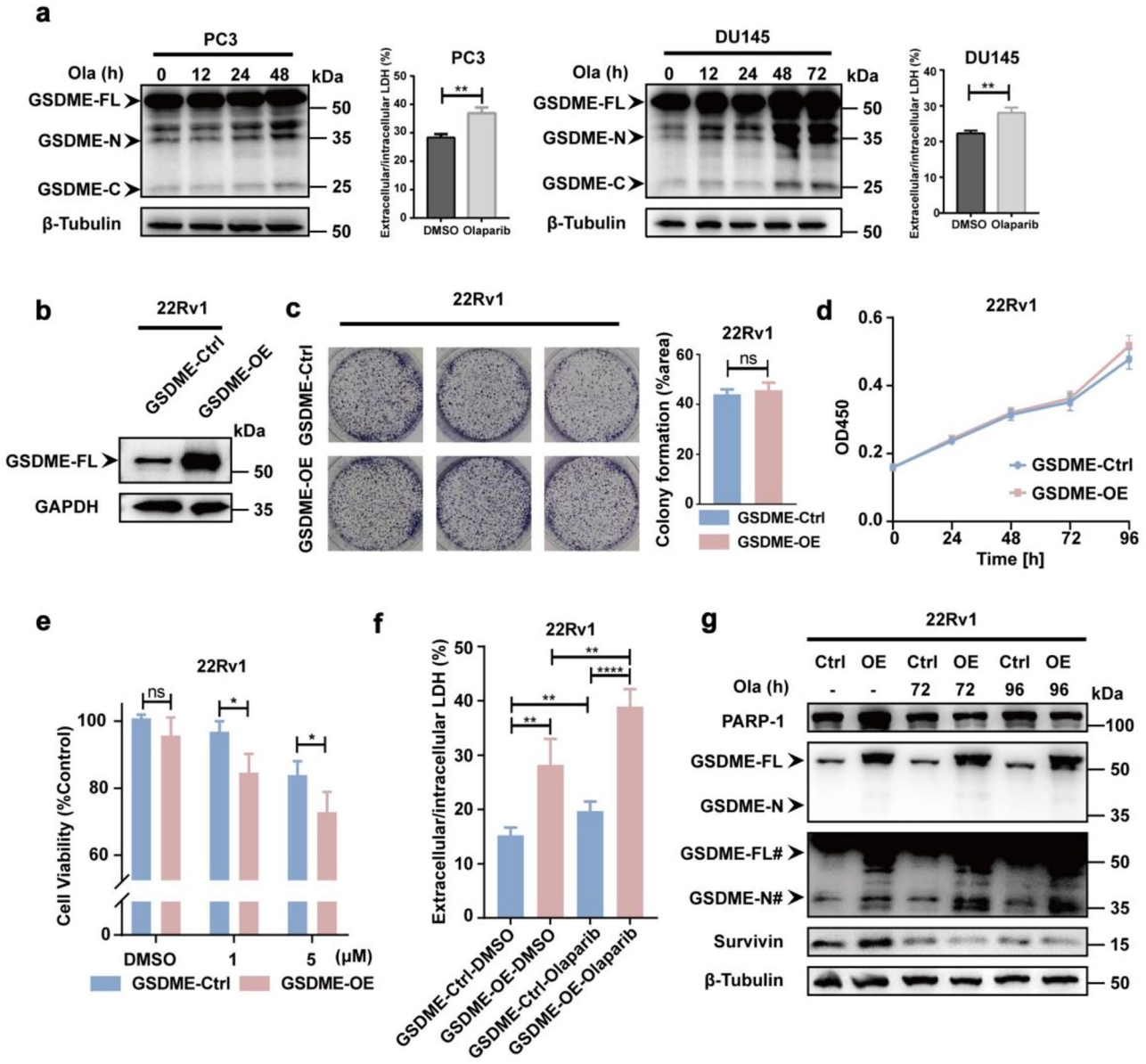

Fig. 3 The overexpression of GSDME increases olaparib response in vitro. **(a)** Proteins were extracted from PC3 and DU145 cells, treated with 5 μM olaparib for indicated time. The expression of GSDME was analyzed by western blotting and the total release levels of LDH was assessed. **(b)** Protein levels of GSDME were analyzed in control (GSDME-Ctrl) and GSDME overexpressed (GSDM-OE) 22Rv1 cells respectively. **(c)** The colony formation assay was performed over 96 h in GSDEM-Ctrl and GSDME-OE 22Rv1 cells (left) and quantification (right). Two-sided unpaired t-test. **(d)** Cell viability based on the CCK-8 assay in the GSDME-Ctrl and GSDME-OE 22Rv1 cells. **(e)** Different tests of GSDME-Ctrl and GSDME-OE 22Rv1 cells treated with indicated DMSO or olaparib for 96 h. Two-sided unpaired t-test. **(f)** The same number of GSDME-Ctrl and GSDME-OE 22Rv1 cells were evaluated for total LDH release levels after 96 h treatment with DMSO and 5 μM olaparib, respectively. **(g)** Western blot of GSDME-Ctrl and GSDME-OE 22Rv1 cells after treatment with 10 μM for 0, 72 and 96 h respectively. ## represents longer exposure. Error bars are expressed as mean ± SEM. $*p<0.05$, $**p<0.01$, $****p<0.0001$

In order to validate the demethylation properties of decitabine in PCa cells, we conducted targeted next-generation bisulfite sequencing analysis on the GSDME promoter region in cultured 22Rv1 cells following treatment with olaparib and decitabine. Compared to untreated cells, our analysis revealed that the significant reduction in methylation levels at representative CpG sites within this region in drug-treated cells (Fig. 4g). These observations provide compelling evidence for the ability of decitabine to induce demethylation in PCa cells. We next assessed the significance of our findings in patients affected by PCa. We roughly identified that 84 prostate cancer patients who harbor HRR gene-mutated and low GSDME expression might benefit from this new treatment strategy in the 489

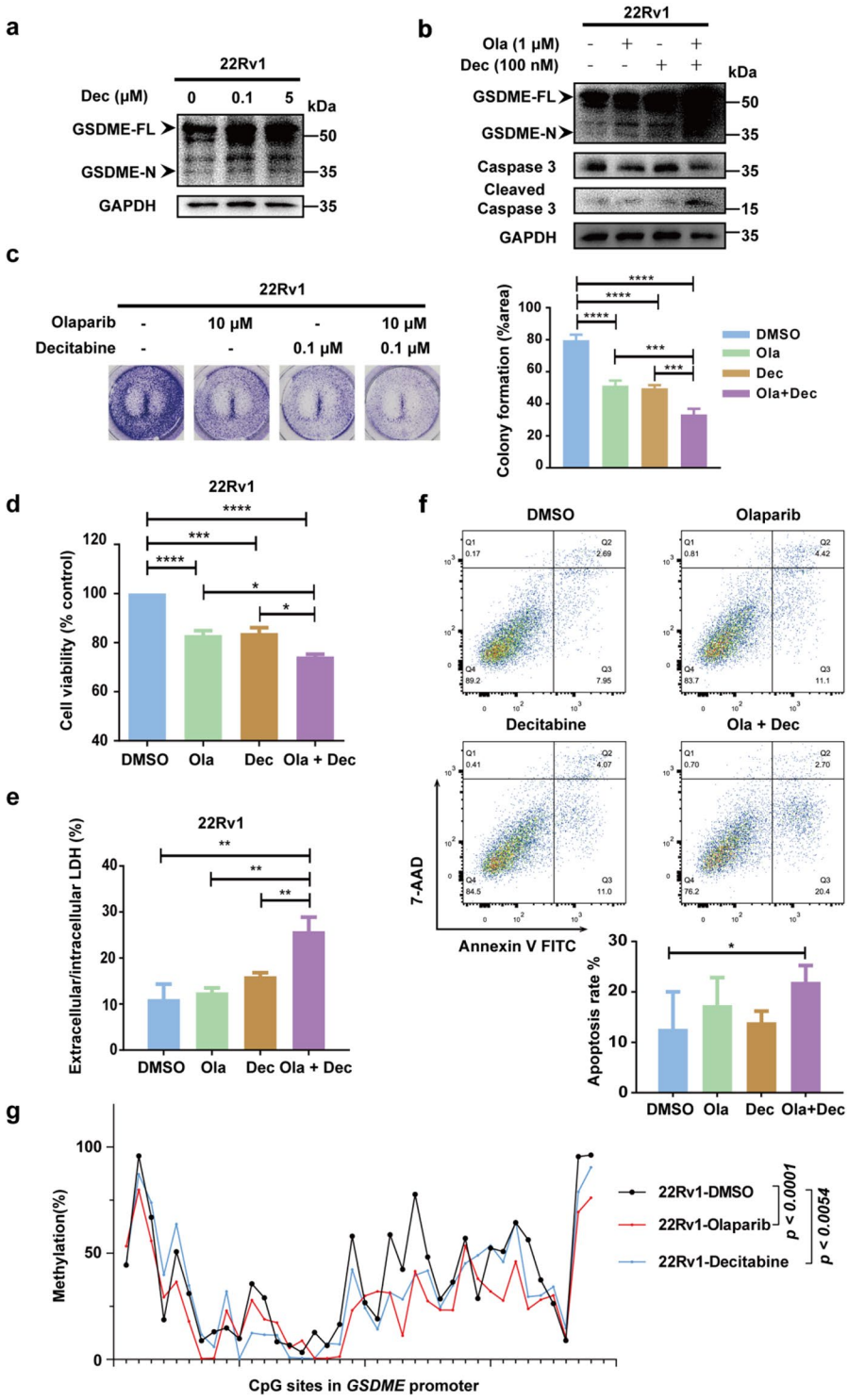

Fig. 4 Decitabine demethylation of GSDME potentiates the therapeutic efficacy of olaparib. **(a)** 22Rv1 cells were treated with DMSO or the 0.1 and 5 μM doses of decitabine for 96 h. The expression level of GSDME was analyzed by western blotting. **(b)** 22Rv1 cells were treated with DMSO, 1 μM olaparib and/or 100 nM decitabine for 96 h. The expression levels of different proteins were analyzed by western blotting. **(c)** The colony formation using DMSO, 10 μM olaparib, 0.1 μM decitabine or indicated olaparib and/or decitabine on 22Rv1 cells for 96 h (upper) and quantification (lower). two-sided unpaired t-test. **(d)** Cell viability based on the CCK-8 assay in 22Rv1 cells were treated for 96 h. **(e)** The total release levels of LDH were represented by the ratio of extracellular to intracellular in 22Rv1 cells after the indicated treatment tests. **(f)** Annexin V^+ cells were analyzed after 22Rv1 cells were treated with DMSO, 5 μM olaparib and/or 5 μM decitabine (upper) and quantification (lower). **(g)** The locations of representative 38 CpG sites analyzed in the GSDME promoter and the percentage of methylation on each CpG site as determined by bisulfite sequencing of 22Rv1 cells after 10μM olaparib and 0.1μM decitabine treatment tests for 96 h. The p value was determined two-sided paired t-test. Error bars are expressed as mean ± SEM, $*p<0.05$, $**p<0.01$, $***p<0.001$, $****p<0.0001$

cases of PanCancer Atlas cohort (Supplementary Fig. S4). The combination of olaparib and decitabine exhibited a potent synergistic therapeutic effect on PCa by promoting the occurrence of pyroptosis in vitro, which supports that the induction of pyroptosis via the combined treatment of olaparib and decitabine represents a promising therapeutic strategy for the treatment of PCa.

3.5 Decitabine increases the efficacy of olaparib therapy in vivo

To assess the functional impact of combination therapy on tumor progression in vivo, we established a xenograft mouse model via subcutaneous injection of 22Rv1 cells into the right flank of nude mice. The animals were then subjected to therapeutic intervention according to the experimental protocol outlined in Fig. 5a. Notably, the combinatorial treatment did not result in significant changes in body weight of the tumor-bearing mice, which indicated that the doses of the interventions were well-tolerated by nude mice (Fig. 5b).We further validated our findings in 22Rv1 xenografts, and showed that the combined treatment with activated caspase-3 to cleave GSDME resulted in reduced tumor volume compared to single-agent treatment. Moreover, co-treatment with olaparib and decitabine led to a significant reduction in tumor cell proliferation as evidenced by decreased expression levels of the anti-apoptotic proteins survivin and BCL-2 (Fig. 5c-f). Taken together, our data demonstrate that decitabine potentiates the antitumor efficacy of olaparib and induces pyroptosis-dependent cell death in PCa. These findings support the development of combinatorial therapies to target the epigenetic regulation pathway and induce pyroptosis for the treatment of PCa.

4 Discussion

In this study, we showed that GSDME expression levels were decreased in PCa, and found that its expression is negatively correlated with methylation levels in PCa. We demonstrated that the clinical agent olaparib induced pyroptosis through caspase-3 cleavage of GSDME, which could be further potentiated by overexpression of GSDME. Furthermore, we discovered that the DNA methyltransferase inhibitor decitabine rescued the epigenetic silencing of GSDME and enhanced synergistically the anti-tumor effect of olaparib. Our investigation emphasizes a pivotal role for GSDME in PCa (Fig. 6).

In recent years, the increasing evidence has highlighted the role of pyroptosis and GSDME in generating vulnerability to cancer therapy. Several studies have found that the level of promoter hypermethylation can ubiquitously restrain GSDME expression, which made GSDME to sever as a promising candidate biomarker for diagnosis, prognosis and therapeutic purposes in various cancers, including gastric [16], hepatocellular [19], colorectal [37] and breast [27] tumors. However, the regulation of GSDME is not always determined solely by epigenetic suppression or loss-of-function mutations. In one illuminating case, GSDME was found to act as a tumor-promoting factor in pancreatic ductal adenocarcinoma (PDAC) by trafficking transcription factor YBX1 into the nucleus to promote membrane-associated mucin expression and protect cancer cells against cytolysis by digestive enzymes [38]. Soon after, interestingly, additional reports have confirmed that USP48, a deubiquitinating enzyme, reduces the degradation of GSDME through deubiquitylation and ultimately induces pyroptosis in PDAC [39]. Noteworthy, these evidences have extended the understanding of diverse functions of GSDME in cancer. Despite the growing body of research on GSDME and pyroptosis in various cancers, little is known about the mechanism of GSDME-mediated pyroptosis in PCa.

Complementarily, we have demonstrated that GSDME is expressed at low levels in PCa due to promoter hypermethylation, which is strongly correlated with poor prognosis. Our study utilized next-generation bisulfite sequencing analysis on all CpG sites within the GSDME promoter to confirm our findings across multiple PCa cohorts in vitro. These results provide robust evidence for the pervasive epigenetic silencing of GSDME in PCa through promoter hypermethylation. Our observations are consistent with previous studies on colorectal cancer tissues, where GSDME levels remain low due to pervasive promoter hypermethylation, while this pattern is reversed in normal tissues with hypomethylated CpG sites in the gene ontology [14]. These observations suggest that aberrant regulation of GSDME expression may play a crucial role in tumorigenesis and subsequently lead to loss of tumor suppression activity. Thus, future studies should focus on identifying the regulatory pathways that manipulating GSDME expression and investigating the role of GSDME in PCa progression.

Olaparib, a third-generation PARP inhibitor, has been approved by the FDA for clinical treatment of CRPC patients [40]. Mechanistically, olaparib involves trapping PARP enzymes to induce DNA single-strand damage, which in turn leads to DNA double-strand damage and synthetic lethality in cancer cells harboring HRR-associated gene mutations (e.g., breast, ovarian, and prostate cancer) [41]. Recent studies have shed new light on the anti-tumor mechanisms of olaparib and revealed its ability to inhibit tumor initiation through DNA damage triggered by innate immunity [42] and senescence [43]. Additionally, talazoparib, another third-generation PARP inhibitor, induce pyroptosis in BRCA1 mutant, but not wild-type, ovarian cancer

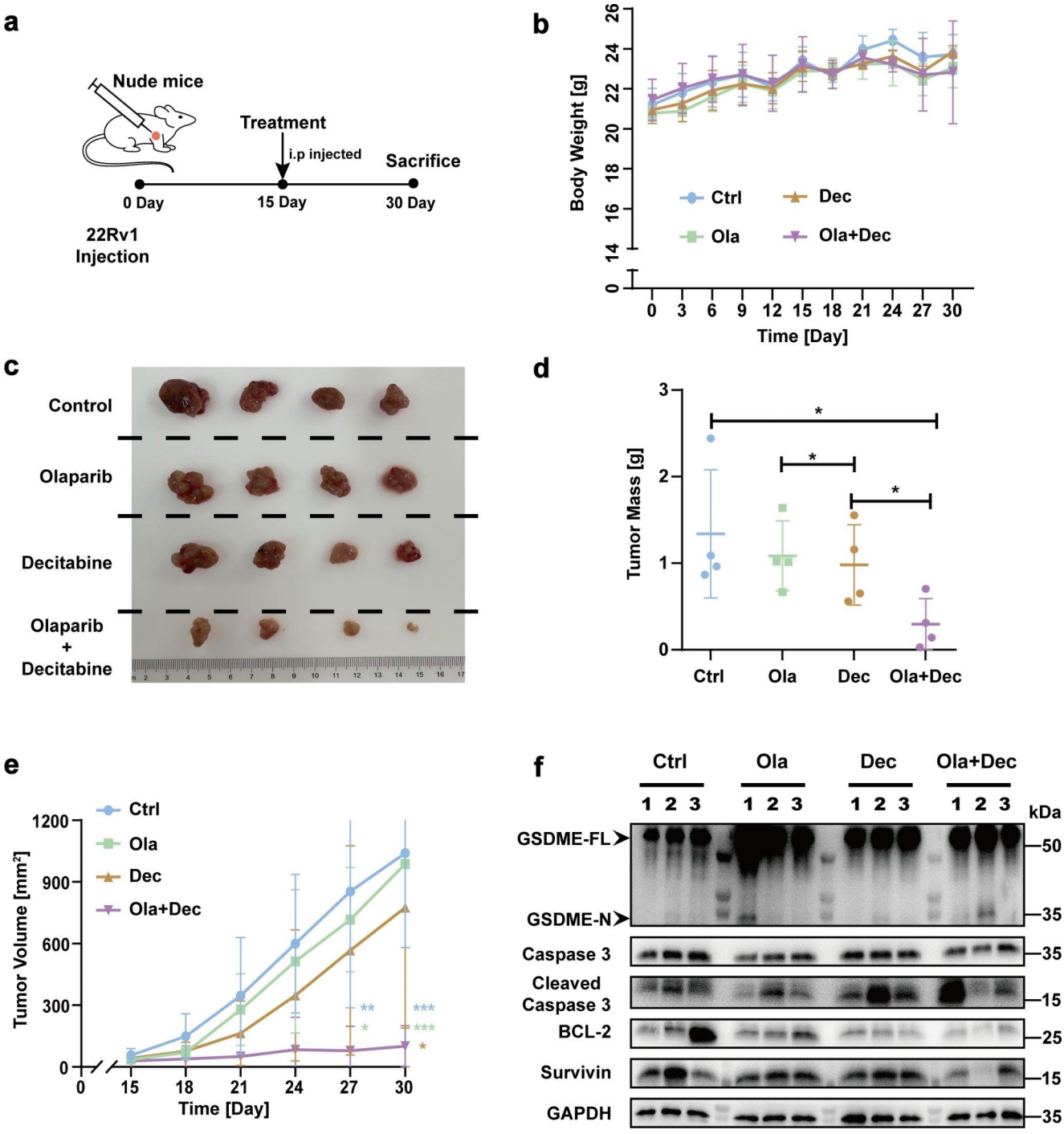

Fig. 5 A novel regimen benefits of combining olaparib and decitabine in vivo. **(a)** Experimental scheme. Briefly, immunodeficient nude male mice were challenged subcutaneously with 22Rv1 cells. The formation of tumor was conspicuous after 15 days and treatments started on day 16. **(b)** Body weight changes of the nude mice in treatment regimen: control (Ctrl), decitabine (Dec), olaparib (Ola) and olaparib plus decitabine (Ola + Dec). ($n = 4$ mice per group). **(c)** Tumor of 22Rv1 allografts were photographed and weighed **(d)** under the indicated treatments. **(e)** Tumor growth of 22Rv1 PCa cells in the flank immunodeficient nude mice ($n = 4$ mice per group). **(f)** Immunoblot analysis of the indicated proteins in tumors after treatment with PBS, olaparib and/or decitabine ($n = 3$ per group). Error bars are expressed as mean ± SEM, $*p < 0.05$, $**p < 0.01$, $**p < 0.01$

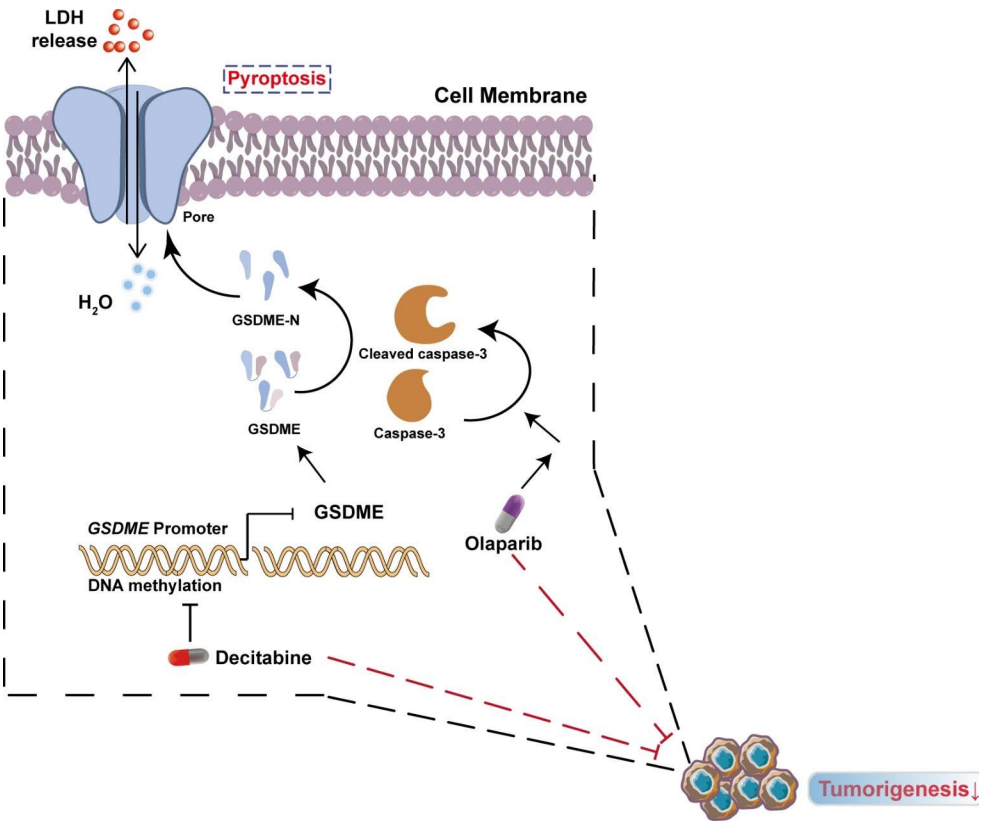

Fig. 6 A model diagram for our study. PCa pathogenesis is characterized by low expression of GSDME that plays a pivotal role in pyroptosis. This phenotype is dependent on epigenetic regulation via DNA methylation, which inhibits the GSDME-mediated cell pyroptosis program and promotes tumor progression. Through targeting aberrant DNA methylation with decitabine, which can restore GSDME expression and promote its cleavage by the clinical therapeutic agent olaparib. This process is mediated through the activation of caspase-3, a key effector molecule in pyroptotic cell death and the cleaved GSDME subsequently causes the release of lactate dehydrogenase (LDH), ultimately rendering tumor regression

cells with intact PARP1 protein binding capacity to DNA by activating caspase-3 cleavage of GSDME at the D270 site [44]. Similarly, we found that olaparib was not limited to the induction of apoptosis, but instead in inducing GSDME cleavage and pyroptosis that was mediated by activation of caspase-3 in a time- and dose-dependent manner in a diverse panel of PCa cell lines. Notably, we also observed that overexpression of GSDME improves the response to olaparib, which may provide a novel therapeutic strategy for PCa patients with limited options. However, further investigations are required to fully elucidate the precise molecular mechanisms underlying the GSDME-mediated sensitivity to PARP inhibitors. Undeniably, our findings, along with those of other researchers, highlight that the potential clinical significance of exploiting PARP inhibitors as a new treatment option for inducing pyroptosis in cancer cells via an alternative cell death pathway.

Notwithstanding that PARP inhibitors have benefited the majority of PCa patients as a breakthrough therapy, but the hurdle of drug resistance in patients who have been prolonged survival has resulted in poor responses to PARP inhibitors [9]. The combination therapy is a currently general tactic to tackle resistance to PARP inhibitors (e.g., immune checkpoint inhibitors) [45]. However, the validated combination strategies remain limited, therefore the exploitation of therapeutic regimens that olaparib exerts a long-term effective response will be an important step. DNA methylation, an epigenetic pattern that manipulates gene in silence without altering the DNA coding sequence, is frequently reported, especially in the promoter region of tumor suppressor gene sequences (e.g., *GSDME*) [46]. A broad array of preclinical and clinical analyses shed light on the role of the regulatory paradigm in primary, metastatic, and neuroendocrine prostate cancer [47, 48]. The combination of drugs targeting DNA methylation with enzalutamide, which are applied in either ongoing (NCT05037500) or completed (NCT00384839) clinical trials to treat patients who suffer from the different stages of PCa. Recently, the synergistic treatment strategy of decitabine in combination with olaparib has been widely noted in a variety of diseases, including cancer [49–51]. One possible mechanism is that decitabine in combination with the olaparib blocks base excision repair (BER) induced by 5-azadC and leads to a synergistic induction of cell death as shown in a panel of Acute Myeloid Leukemia (AML) cells [50]. Our study opens a novel regimen of the combination olaparib with decitabine for the therapeutic targeting of PCa. Our results also support the notion that, in PRAD, both activation of pyroptosis and demethylation of the promoter of GSDME CpG sites should be desired to improve the efficacy of clinical therapy. Nonetheless, a comprehensive understanding of the molecular mechanisms involves in the new therapy against tumors is crucial and deserves further investigation.

In summary, our results indicate that CpG sites hypermethylation at the GSDME gene promoter might be renders these cells highly amenable to the innovative therapeutic targeting strategies. Importantly, our study reveals that olaparib activates the pyroptosis pathway via a novel caspase-3 cleavage GSDME-dependent mechanism, and ultimately impedes tumor development. Critically, decitabine potentiates the above effect, which further demonstrated the efficacy of combinatorial therapeutic approaches in preclinical mouse models. Overall, our findings underscore that the potential utility of GSDME serve as a detectable and prognostic biomarker, and highlight that the promise of novel therapeutic strategies to target GSDME-mediated pathways for the treatment of PCa.

Supplementary Information The online version contains supplementary material available at https://doi.org/10.1007/s13402-023-00860-3.

Acknowledgements We appreciated the free access to TCGA, GEO, DNMIVD and EWAS Data Hub databases and GSEA software.

Authors' contributions T.W. conceived and designed the experiments. T.W. and A.T. performed the experiments, acquired, and analyzed data, presented figures, and wrote manuscript of the paper. Y.Z. and J.C. performed the experiments and analyzed the data. J.S. provided the clinical-related materials. W.X. acquired fundings and supervised experiments. W.X. conceived and designed the experiments, reviewed drafts of the paper, and approved the final draft.

Funding This work was supported by grants from Ministry of Science and Technology (2022YFC2702703), Science and Technology Commission of Shanghai Municipality (21ZR1433100), and SJTU funding (YG2022ZD016).

Declarations

Ethics approval and consent to participate Ethics committee approval from School of Biomedical Engineering, Shanghai Jiao Tong University (Shanghai, China) was obtained prior to the research and informed written consent of all participants were obtained. All animal studies were performed following the Institutional Ethics Committee of School of Biomedical Engineering, Shanghai Jiao Tong University (Shanghai, China).

Competing interests The authors declare no competing interests.

References

1. H. Sung, J. Ferlay, R.L. Siegel, M. Laversanne, I. Soerjomataram, A. Jemal, F. Bray, Global Cancer Statistics 2020, GLOBOCAN estimates of incidence and Mortality Worldwide for 36 cancers in 185 countries. CA Cancer J Clin. **71**, 209–249 (2021)
2. R.L. Siegel, K.D. Miller, H.E. Fuchs, A. Jemal, Cancer statistics, 2022. CA Cancer J Clin. **72**, 7–33 (2022)
3. C. Tran, S. Ouk, N.J. Clegg, Y. Chen, P.A. Watson, V. Arora, J. Wongvipat, P.M. Smith-Jones, D. Yoo, A. Kwon, T. Wasielewska, D. Welsbie, C.D. Chen, C.S. Higano, T.M. Beer, D.T. Hung, H.I. Scher, M.E. Jung, C.L. Sawyers, Development of a second-generation antiandrogen for treatment of advanced prostate cancer. Science. **324**, 787–790 (2009)
4. A.H. Davies, H. Beltran, A. Zoubeidi, Cellular plasticity and the neuroendocrine phenotype in prostate cancer. Nat. Rev. Urol. **15**, 271–286 (2018)
5. D. Robinson, E.M. Van Allen, Y.M. Wu, N. Schultz, R.J. Lonigro, J.M. Mosquera, B. Montgomery, M.E. Taplin, C.C. Pritchard, G. Attard, H. Beltran, W. Abida, R.K. Bradley, J. Vinson, X.H. Cao, P. Vats, L.P. Kunju, M. Hussain, F.Y. Feng, S.A. Tomlins, K.A. Cooney, D.C. Smith, C. Brennan, J. Siddiqui, R. Mehra, Y. Chen, D.E. Rathkopf, M.J. Morris, S.B. Solomon, J.C. Durack, V.E. Reuter, A. Gopalan, J.J. Gao, M. Loda, R.T. Lis, M. Bowden, S.P. Balk, G. Gaviola, C. Sougnez, M. Gupta, E.Y. Yu, E.A. Mostaghel, H.H. Cheng, H. Mulcahy, L.D. True, S.R. Plymate, H. Dvinge, R. Ferraldeschi, P. Flohr, S. Miranda, Z. Zafeiriou, N. Tunariu, J. Mateo, R. Perez-Lopez, F. Demichelis, B.D. Robinson, M. Schiffman, D.M. Nanus, S.T. Tagawa, A. Sigaras, K.W. Eng, O. Elemento, A. Sboner, E.I. Heath, H.I. Scher, K.J. Pienta, P. Kantoff, J.S. de Bono, M.A., P.S. Rubin, Nelson, L.A., Garraway, C.L. Sawyers and A.M. Chinnaiyan, Integrative Clinical Genomics of Advanced Prostate Cancer. Cell. 161, 1215–1228 (2015)
6. J. Mateo, S. Carreira, S. Sandhu, S. Miranda, H. Mossop, R. Perez-Lopez, D. Nava Rodrigues, D. Robinson, A. Omlin, N. Tunariu, G. Boysen, N. Porta, P. Flohr, A. Gillman, I. Figueiredo, C. Paulding, G. Seed, S. Jain, C. Ralph, A. Protheroe, S. Hussain, R. Jones, T. Elliott, U. McGovern, D. Bianchini, J. Goodall, Z. Zafeiriou, C.T. Williamson, R. Ferraldeschi, R. Riisnaes, B. Ebbs, G. Fowler, D. Roda, W. Yuan, Y.M. Wu, X. Cao, R. Brough, H. Pemberton, R. A'Hern, A. Swain, L.P. Kunju, R. Eeles, G. Attard, C.J. Lord, A. Ashworth, M.A. Rubin, K.E. Knudsen, F.Y. Feng, A.M. Chinnaiyan, Hall and J.S. de Bono, DNA-Repair defects and Olaparib in metastatic prostate Cancer. N Engl. J. Med. **373**, 1697–1708 (2015)
7. J. de Bono, J. Mateo, K. Fizazi, F. Saad, N. Shore, S. Sandhu, K.N. Chi, O. Sartor, N. Agarwal, D. Olmos, A. Thiery-Vuillemin, P. Twardowski, N. Mehra, C. Goessl, J. Kang, J. Burgents, W. Wu, A. Kohlmann, C.A. Adelman, M. Hussain, Olaparib for metastatic castration-resistant prostate Cancer. N Engl. J. Med. **382**, 2091–2102 (2020)
8. M. Hussain, J. Mateo, K. Fizazi, F. Saad, N. Shore, S. Sandhu, K.N. Chi, O. Sartor, N. Agarwal, D. Olmos, A. Thiery-Vuillemin, P. Twardowski, G. Roubaud, M. Ozguroglu, J. Kang, J. Burgents, C. Gresty, C. Corcoran, C.A. de Adelman, Bono and P.R.T. investigators, survival with Olaparib in Metastatic Castration-Resistant prostate Cancer. N Engl. J. Med. **383**, 2345–2357 (2020)
9. M.P. Dias, S.C. Moser, S. Ganesan, J. Jonkers, Understanding and overcoming resistance to PARP inhibitors in cancer therapy. Nat. Rev. Clin. Oncol. **18**, 773–791 (2021)
10. G. van Camp, P. Coucke, W. Balemans, D. van Velzen, C. van de Bilt, L. van Laer, R.J. Smith, K. Fukushima, G.W. Padberg, R.R. Frants, Localization of a gene for non-syndromic hearing loss (DFNA5) to chromosome 7p15. Hum. Mol. Genet. **4**, 2159–2163 (1995)
11. L. Galluzzi, I. Vitale, S.A. Aaronson, J.M. Abrams, D. Adam, P. Agostinis, E.S. Alnemri, L. Altucci, I. Amelio, D.W. Andrews, M. Annicchiarico-Petruzzelli, A.V. Antonov, E. Arama, E.H. Baehrecke, N.A. Barlev, N.G. Bazan, F. Bernassola, M.J.M. Bertrand, K. Bianchi, M.V. Blagosklonny, K. Blomgren, C. Borner, P. Boya, C. Brenner, M. Campanella, E. Candi, D. Carmona-Gutierrez, F. Cecconi, F.K. Chan, N.S. Chandel, E.H. Cheng, J.E. Chipuk, J.A. Cidlowski, A. Ciechanover, G.M. Cohen, M. Conrad, J.R. Cubillos-Ruiz, P.E. Czabotar, V. D'Angiolella, T.M. Dawson, V.L. Dawson, V. De Laurenzi, R. De Maria, K.M. Debatin, R.J. DeBerardinis, M. Deshmukh, N. Di Daniele, F. Di Virgilio, V.M.

Dixit, S.J. Dixon, C.S. Duckett, B.D. Dynlacht, W.S. El-Deiry, J.W. Elrod, G.M. Fimia, S. Fulda, A.J. Garcia-Saez, A.D. Garg, C. Garrido, E. Gavathiotis, P. Golstein, E. Gottlieb, D.R. Green, L.A. Greene, H. Gronemeyer, A. Gross, G. Hajnoczky, J.M. Hardwick, I.S. Harris, M.O. Hengartner, C. Hetz, H. Ichijo, M. Jaattela, B. Joseph, P.J. Jost, P.P. Juin, W.J. Kaiser, M. Karin, T. Kaufmann, O. Kepp, A. Kimchi, R.N. Kitsis, D.J. Klionsky, R.A. Knight, S. Kumar, S.W. Lee, J.J. Lemasters, B. Levine, A. Linkermann, S.A. Lipton, R.A. Lockshin, C. Lopez-Otin, S.W. Lowe, T. Luedde, E. Lugli, M. MacFarlane, F. Madeo, M. Malewicz, W. Malorni, G. Manic, J.C. Marine, S.J. Martin, J.C. Martinou, J.P. Medema, P. Mehlen, P. Meier, S. Melino, E.A. Miao, J.D. Molkentin, U.M. Moll, C. Munoz-Pinedo, S. Nagata, G. Nunez, A. Oberst, M. Oren, M. Overholtzer, M. Pagano, T. Panaretakis, M. Pasparakis, J.M. Penninger, D.M. Pereira, S. Pervaiz, M.E. Peter, M. Piacentini, P. Pinton, J.H.M. Prehn, H. Puthalakath, G.A. Rabinovich, M. Rehm, R. Rizzuto, C.M.P. Rodrigues, D.C. Rubinsztein, T. Rudel, K.M. Ryan, E. Sayan, L. Scorrano, F. Shao, Y. Shi, J. Silke, H.U. Simon, A. Sistigu, B.R. Stockwell, A. Strasser, G. Szabadkai, S.W.G. Tait, D. Tang, N. Tavernarakis, A. Thorburn, Y. Tsujimoto, B. Turk, T. Vanden Berghe, P. Vandenabeele, M.G. Vander Heiden, A. Villunger, H.W. Virgin, K.H. Vousden, D. Vucic, E.F. Wagner, H. Walczak, D. Wallach, Y. Wang, J.A. Wells, W. Wood, J. Yuan, Z. Zakeri, B. Zhivotovsky, L. Zitvogel, G. Melino and G. Kroemer, Molecular mechanisms of cell death: recommendations of the Nomenclature Committee on Cell Death 2018. Cell Death Differ. **25**, 486–541 (2018)

12. Z. Zhang, Y. Zhang, S. Xia, Q. Kong, S. Li, X. Liu, C. Junqueira, K.F. Meza-Sosa, T.M.Y. Mok, J. Ansara, S. Sengupta, Y. Yao, H. Wu, J. Lieberman, Gasdermin E suppresses tumour growth by activating anti-tumour immunity. Nature. **579**, 415–420 (2020)
13. Y.P. Wang, W.Q. Gao, X.Y. Shi, J.J. Ding, W. Liu, H.B. He, K. Wang, F. Shao, Chemotherapy drugs induce pyroptosis through caspase-3 cleavage of a gasdermin. Nature. **547**, 99–103 (2017)
14. J. Ibrahim, K.O. de Beeck, E. Fransen, L. Croes, M. Beyens, A. Suls, W. Vanden Berghe, M. Peeters, G. Van Camp, Methylation analysis of Gasdermin E shows great promise as a biomarker for colorectal cancer. Cancer Med-Us. **8**, 2133–2145 (2019)
15. M.S. Kim, X. Chang, K. Yamashita, J.K. Nagpal, J.H. Baek, G. Wu, B. Trink, E.A. Ratovitski, M. Mori, D. Sidransky, Aberrant promoter methylation and tumor suppressive activity of the DFNA5 gene in colorectal carcinoma. Oncogene. **27**, 3624–3634 (2008)
16. K. Akino, M. Toyota, H. Suzuki, T. Imai, R. Maruyama, M. Kusano, N. Nishikawa, Y. Watanabe, Y. Sasaki, T. Abe, E. Yamamoto, I. Tarasawa, T. Sonoda, M. Mori, K. Imai, Y. Shinomura, T. Tokino, Identification of DFNA5 as a target of epigenetic inactivation in gastric cancer. Cancer Sci. **98**, 88–95 (2007)
17. M. Katoh, M. Katoh, Identification and characterization of human DFNA5L, mouse Dfna5l, and rat Dfna5l genes in silico. Int. J. Oncol. **25**, 765–770 (2004)
18. Y. Zhang, J. Yang, Z. Wen, X. Chen, J. Yu, D. Yuan, B. Xu, H. Luo, J. Zhu, A novel 3',5'-diprenylated chalcone induces concurrent apoptosis and GSDME-dependent pyroptosis through activating PKCdelta/JNK signal in prostate cancer. Aging (Albany NY). **12**, 9103–9124 (2020)
19. C.J. Wang, L. Tang, D.W. Shen, C. Wang, Q.Y. Yuan, W. Gao, Y.K. Wang, R.H. Xu, H. Zhang, The expression and regulation of DFNA5 in human hepatocellular carcinoma DFNA5 in hepatocellular carcinoma. Mol. Biol. Rep. **40**, 6525–6531 (2013)
20. J. Yu, B. Qin, A.M. Moyer, S. Nowsheen, T. Liu, S. Qin, Y. Zhuang, D. Liu, S.W. Lu, K.R. Kalari, D.W. Visscher, J.A. Copland, S.A. McLaughlin, A. Moreno-Aspitia, D.W. Northfelt, R.J. Gray, Z. Lou, V.J. Suman, R. Weinshilboum, J.C. Boughey, M.P. Goetz, L. Wang, DNA methyltransferase expression in triple-negative breast cancer predicts sensitivity to decitabine. J. Clin. Invest. **128**, 2376–2388 (2018)
21. E. Kaminskas, A. Farrell, S. Abraham, A. Baird, L.S. Hsieh, S.L. Lee, J.K. Leighton, H. Patel, A. Rahman, R. Sridhara, Y.C. Wang, Pazdur and Fda, approval summary: azacitidine for treatment of myelodysplastic syndrome subtypes. Clin. Cancer Res. **11**, 3604–3608 (2005)
22. C. Rogers, T. Fernandes-Alnemri, L. Mayes, D. Alnemri, G. Cingolani, E.S. Alnemri, Cleavage of DFNA5 by caspase-3 during apoptosis mediates progression to secondary necrotic/pyroptotic cell death. Nat. Commun. **8**, 14128 (2017)
23. A. Subramanian, P. Tamayo, V.K. Mootha, S. Mukherjee, B.L. Ebert, M.A. Gillette, A. Paulovich, S.L. Pomeroy, T.R. Golub, E.S. Lander, J.P. Mesirov, Gene set enrichment analysis: a knowledge-based approach for interpreting genome-wide expression profiles. Proc. Natl. Acad. Sci. U S A **102**, 15545–15550 (2005)
24. V.K. Mootha, C.M. Lindgren, K.F. Eriksson, A. Subramanian, S. Sihag, J. Lehar, P. Puigserver, E. Carlsson, M. Ridderstrale, E. Laurila, N. Houstis, M.J. Daly, N. Patterson, J.P. Mesirov, T.R. Golub, P. Tamayo, B. Spiegelman, E.S. Lander, J.N. Hirschhorn, D. Altshuler, L.C. Groop, PGC-1alpha-responsive genes involved in oxidative phosphorylation are coordinately downregulated in human diabetes. Nat. Genet. **34**, 267–273 (2003)
25. W. Ding, G. Feng, Y. Hu, G. Chen, T. Shi, Co-occurrence and mutual exclusivity analysis of DNA methylation reveals distinct subtypes in multiple cancers. Front. Cell. Dev. Biol. **8**, 20 (2020)
26. Z. Xiong, F. Yang, M. Li, Y. Ma, W. Zhao, G. Wang, Z. Li, X. Zheng, D. Zou, W. Zong, H. Kang, Y. Jia, R. Li, Z. Zhang, Y. Bao, EWAS Open platform: integrated data, knowledge and toolkit for epigenome-wide association study. Nucleic Acids Res. **50**, D1004–D1009 (2022)
27. L. Croes, M. Beyens, E. Fransen, J. Ibrahim, W.V. Berghe, A. Suls, M. Peeters, P. Pauwels, G. Van Camp, K.O. de Beeck, Large-scale analysis of DFNA5 methylation reveals its potential as biomarker for breast cancer. Clin. Epigenetics. **10**, 51 (2018)
28. J. Hu, F.J. Sanchez-Rivera, Z. Wang, G.N. Johnson, Y.J. Ho, K. Ganesh, S. Umeda, S. Gan, A.M. Mujal, R.B. Delconte, J.P. Hampton, H. Zhao, S. Kottapalli, E. de Stanchina, C.A. Iacobuzio-Donahue, D. Pe'er, S.W. Lowe, J.C. Sun, J. Massague, STING inhibits the reactivation of dormant metastasis in lung adenocarcinoma. Nature. **616**, 806–813 (2023)
29. D.A. Moser, S. Muller, E.M. Hummel, A.S. Limberg, L. Dieckmann, L. Frach, J. Pakusch, V. Flasbeck, M. Brune, J. Beygo, L. Klein-Hitpass, R. Kumsta, Targeted bisulfite sequencing: a novel tool for the assessment of DNA methylation with high sensitivity and increased coverage. Psychoneuroendocrinology. **120**, 104784 (2020)
30. Y. Zhang, T. Wu, Y. Wang, Z. Chen, J. Chen, S. Lu, W. Xia, Reciprocal FGF19-GLI2 signaling induces epithelial-to-mesenchymal transition to promote lung squamous cell carcinoma metastasis. Cell. Oncol. **46**, 437–450 (2023)
31. Y. Zhang, T. Wu, F. Li, Y. Cheng, Q. Han, X. Lu, S. Lu, W. Xia, FGF19 is Coamplified with CCND1 to promote proliferation in lung squamous cell carcinoma and their combined inhibition shows improved efficacy. Front. Oncol. **12**, 846744 (2022)
32. Q. Han, Q.R. Xie, F. Li, Y. Cheng, T. Wu, Y. Zhang, X. Lu, A.S.T. Wong, J. Sha, W. Xia, Targeted inhibition of SIRT6 via engineered exosomes impairs tumorigenesis and metastasis in prostate cancer. Theranostics. **11**, 6526–6541 (2021)
33. W. Gong, P. Fang, M. Leng, Y. Shi, Promoting GSDME expression through DNA demethylation to increase chemosensitivity of breast cancer MCF-7 / taxol cells. Plos One **18**, e0282244 (2023)
34. X. Wei, F. Xie, X. Zhou, Y. Wu, H. Yan, T. Liu, J. Huang, F. Wang, F. Zhou, L. Zhang, Role of pyroptosis in inflammation and cancer. Cell. Mol. Immunol. **19**, 971–992 (2022)

35. J. Armenia, S.A.M. Wankowicz, D. Liu, J. Gao, R. Kundra, E. Reznik, W.K. Chatila, D. Chakravarty, G.C. Han, I. Coleman, B. Montgomery, C. Pritchard, C. Morrissey, C.E. Barbieri, H. Beltran, A. Sboner, Z. Zafeiriou, S. Miranda, C.M. Bielski, A.V. Penson, C. Tolonen, F.W. Huang, D. Robinson, Y.M. Wu, R. Lonigro, L.A. Garraway, F. Demichelis, P.W. Kantoff, M.E. Taplin, W. Abida, B.S. Taylor, H.I. Scher, P.S. Nelson, J.S. de Bono, M.A. Rubin, C.L. Sawyers, A.M. Chinnaiyan, P.S.C.I.P.C.D. Team, N. Schultz and E.M. Van Allen, the long tail of oncogenic drivers in prostate cancer. Nat. Genet. **50**, 645–651 (2018).
36. P.A. Jones, S.M. Taylor, Cellular differentiation, cytidine analogs and DNA methylation. Cell. **20**, 85–93 (1980)
37. K. Yokomizo, Y. Harada, K. Kijima, K. Shinmura, M. Sakata, K. Sakuraba, Y. Kitamura, A. Shirahata, T. Goto, H. Mizukami, M. Saito, G. Kigawa, H. Nemoto, K. Hibi, Methylation of the DFNA5 gene is frequently detected in Colorectal Cancer. Anticancer Res. **32**, 1319–1322 (2012)
38. J. Lv, Y. Liu, S. Mo, Y. Zhou, F. Chen, F. Cheng, C. Li, D. Saimi, M. Liu, H. Zhang, K. Tang, J. Ma, Z. Wang, Q. Zhu, W.M. Tong, B. Huang, Gasdermin E mediates resistance of pancreatic adenocarcinoma to enzymatic digestion through a YBX1-mucin pathway. Nat. Cell. Biol. **24**, 364–372 (2022)
39. Y. Ren, M. Feng, X. Liu, X. Hao, J. Li, P. Li, J. Gao, Q. Qi, L. Du, C. Wang, Q. Wang, Y. Wang, USP48 stabilizes gasdermin E to promote pyroptosis in cancer. Cancer Res. **83**, 1074–1093 (2023)
40. N.J. Curtin, C. Szabo, Poly(ADP-ribose) polymerase inhibition: past, present and future. Nat. Rev. Drug Discov. **19**, 711–736 (2020)
41. C.J. Lord, A. Ashworth, PARP inhibitors: synthetic lethality in the clinic. Science. **355**, 1152–1158 (2017)
42. C. Kim, X.D. Wang, Y. Yu, PARP1 inhibitors trigger innate immunity via PARP1 trapping-induced DNA damage response. Elife **9**, e60637 (2020)
43. A.P. Lombard, C.M. Armstrong, L.S. D'Abronzo, S. Ning, A.R. Leslie, M. Sharifi, W. Lou, C.P. Evans, M. Dall'Era, H.W. Chen, X. Chen, A.C. Gao, Olaparib-Induced Senescence is bypassed through G2-M checkpoint override in Olaparib-Resistant prostate Cancer. Mol. Cancer Ther. **21**, 677–685 (2022)
44. C. Kim, X.D. Wang, S. Jang, Y. Yu, PARP1 inhibitors induce pyroptosis via caspase 3-mediated gasdermin E cleavage. Biochem. Biophys. Res. Commun. **646**, 78–85 (2023)
45. J. Shen, W. Zhao, Z. Ju, L. Wang, Y. Peng, M. Labrie, T.A. Yap, G.B. Mills, G. Peng, PARPi triggers the STING-Dependent Immune response and enhances the therapeutic efficacy of Immune Checkpoint Blockade Independent of BRCAness. Cancer Res. **79**, 311–319 (2019)
46. A. Kumaraswamy, K.R. Welker Leng, T.C. Westbrook, J.A. Yates, S.G. Zhao, C.P. Evans, F.Y. Feng, T.M. Morgan, J.J. Alumkal, Recent advances in epigenetic biomarkers and epigenetic targeting in prostate Cancer. Eur. Urol. **80**, 71–81 (2021)
47. S.G. Zhao, W.S. Chen, H. Li, A. Foye, M. Zhang, M. Sjostrom, R. Aggarwal, D. Playdle, A. Liao, J.J. Alumkal, R. Das, J. Chou, J.T. Hua, T.J. Barnard, A.M. Bailey, E.D. Chow, M.D. Perry, H.X. Dang, R. Yang, R. Moussavi-Baygi, L. Zhang, M. Alshalalfa, S. Laura Chang, K.E. Houlahan, Y.J. Shiah, T.M. Beer, G. Thomas, K.N. Chi, M. Gleave, A. Zoubeidi, R.E. Reiter, M.B. Rettig, O. Witte, M. Yvonne Kim, L. Fong, D.E. Spratt, T.M. Morgan, R. Bose, F.W. Huang, H. Li, L. Chesner, T. Shenoy, H. Goodarzi, I.A. Asangani, S. Sandhu, J.M. Lang, N.P. Mahajan, P.N. Lara, C.P. Evans, P. Febbo, S. Batzoglou, K.E. Knudsen, H.H. He, J. Huang, W. Zwart, J.F. Costello, J. Luo, S.A. Tomlins, A.W. Wyatt, S.M. Dehm, A. Ashworth, L.A. Gilbert, P.C. Boutros, K. Farh, A.M. Chinnaiyan, C.A. Maher, E.J. Small, D.A. Quigley and F.Y. Feng, The DNA methylation landscape of advanced prostate cancer. Nat Genet. 52, 778–789 (2020)
48. K.E. Houlahan, Y.J. Shiah, A. Gusev, J. Yuan, M. Ahmed, A. Shetty, S.G. Ramanand, C.Q. Yao, C. Bell, E. O'Connor, V. Huang, M. Fraser, L.E. Heisler, J. Livingstone, T.N. Yamaguchi, A. Rouette, A. Foucal, S.M.G. Espiritu, A. Sinha, M. Sam, L. Timms, J. Johns, A. Wong, A. Murison, M. Orain, V. Picard, H. Hovington, A. Bergeron, L. Lacombe, M. Lupien, Y. Fradet, B. Tetu, J.D. McPherson, B. Pasaniuc, T. Kislinger, M.L.K. Chua, M.M. Pomerantz, T. van der Kwast, M.L. Freedman, R.S. Mani, H.H. He, R.G. Bristow, P.C. Boutros, Genome-wide germline correlates of the epigenetic landscape of prostate cancer. Nat. Med. **25**, 1615–1626 (2019)
49. J.I. Shim, J.Y. Ryu, S.Y. Jeong, Y.J. Cho, J.J. Choi, J.R. Hwang, J.Y. Choi, J.K. Sa, J.W. Lee, Combination effect of poly (ADP-ribose) polymerase inhibitor and DNA demethylating agents for treatment of epithelial ovarian cancer. Gynecol. Oncol. **165**, 270–280 (2022)
50. M.L. Orta, A. Höglund, J.M. Calderón-Montaño, I. Domínguez, E. Burgos-Morón, T. Visnes, N. Pastor, C. Ström, M. López-lázaro, T. Helleday, The PARP inhibitor Olaparib disrupts base excision repair of 5-aza-2'-deoxycytidine lesions. Nucleic Acids Res. **42**, 9108–9120 (2014)
51. B.C. Valdez, Y. Li, D. Murray, Y. Liu, Y. Nieto, R.E. Champlin, B.S. Andersson, Combination of a hypomethylating agent and inhibitors of PARP and HDAC traps PARP1 and DNMT1 to chromatin, acetylates DNA repair proteins, down-regulates NuRD and induces apoptosis in human leukemia and lymphoma cells. Oncotarget. **9**, 3908–3921 (2018)

Publisher's Note Springer Nature remains neutral with regard to jurisdictional claims in published maps and institutional affiliations.

Springer Nature or its licensor (e.g. a society or other partner) holds exclusive rights to this article under a publishing agreement with the author(s) or other rightsholder(s); author self-archiving of the accepted manuscript version of this article is solely governed by the terms of such publishing agreement and applicable law.